In vivo amyloid-like fibrils produced under stress

Natália A. Fontana[1], Ariane D. Rosse[1], Anthony Watts[2], Paulo S. R. Coelho[3], Antonio J. Costa-Filho[1,*]

1- Departamento de Física, Faculdade de Filosofia, Ciências e Letras de Ribeirão Preto, Universidade de São Paulo, Ribeirão Preto, SP, Brazil

2- Department of Biochemistry, University of Oxford, Oxford, UK

3- Departamento de Biologia Celular e Molecular e Bioagentes Patogênicos, Faculdade de Medicina de Ribeirão Preto, Universidade de São Paulo, Ribeirão Preto, SP, Brazil

To whom correspondence should be addressed: Antonio J. Costa-Filho, DF/FFCLRP/USP, Av. Bandeirantes 3900, Ribeirão Preto, SP, Brazil, 14040-901, E-mail: ajcosta@usp.br, Phone: +551633153665.

Abstract

The participation of amyloids in neurodegenerative diseases and in functional processes has triggered the quest for methods allowing their direct detection *in vivo*. Despite the plethora of data, those methods are still lacking. We used the autofluorescence from the extended β-sheets of amyloids to follow fibrillation of *S. cerevisiae* Golgi Reassembly and Stacking Protein (Grh1). Grh1 has been implicated in starvation-triggered unconventional protein secretion (UPS) and here we suggest the idea of its participation also in heat shock response (HSR). Fluorescence Lifetime Imaging (FLIM) was used to detect fibril autofluorescence in cells (*E. coli* and yeast) under stress (starvation and higher temperature). The formation of Grh1 large complexes under stress was further supported by size exclusion chromatography and ultracentrifugation. Our data show the first-time *in vivo* detection of amyloids without the use of extrinsic probes as well as bring new perspectives on the participation of Grh1 in UPS and HSR.

Introduction

Amyloid fibrils have been a subject of major interest over the years due to their pivotal participation in several neurodegenerative diseases [1] and, more recently, in functional processes [2]. Although the structural 3D arrangement of the fibrils and factors governing their formation have been thoroughly investigated [3,4], detecting amyloid-like fibrils *in vivo* is still not trivial. Aggregation has been monitored inside cells using GFP-labelled proteins combined with fluorescence methods [5]. The visualization of fibrils has been achieved using methods based on dyes that bind to amyloid plaques in excised brain tissue [6], and *in vivo* diagnostics of neurodegenerative diseases have been reported using Magnetic Resonance Imaging [7]. To directly observe fibrils inside cells, other biochemical and biophysical approaches are still necessary.

Recently, Pinotsi *et al* showed that the formation of amyloid fibrils by tau protein and lysozyme exhibited a characteristic fluorescence in the visible range [8]. The origin of such autofluorescence was attributed to the absorption/emission of electrons delocalized after the formation of hydrogen bonds in the typical β-sheet structure of amyloids, thus allowing low-energy electronic transitions to occur [8,9]. The specific molecular origin of the phenomenon is, however, still not completely understood [9]. Despite this uncertainty, the observed autofluorescence has been firmly correlated with amyloid formation in several cases, such as Amyloid-β [10] and α-synuclein [11]. Nonetheless, fibril formation monitoring was either restricted to the *in vitro* assembly [10] or *in vivo* detection using FRET between an extrinsic probe attached to the protein and the fibril [11].

The use of autofluorescence for direct detection of *in vivo* fibrillation without the use of an extrinsic probe has not been satisfactorily explored. One of the reasons could be the apparent lack of specificity in detecting the fibril signal due to the competing autofluorescence from the cells. Here, we report results on the *in vivo* formation of amyloid-like fibrils by one member of the Golgi Reassembly and Stacking Protein (GRASP) family without the use of an extrinsic dye for protein tagging.

GRASPs were initially implicated as participants in the structural organization of the Golgi apparatus [12], a central organelle in the conventional endoplasmic reticulum (ER)-to-Golgi pathway of protein secretion [13]. However, proteins can reach

the plasma membrane and/or leave the cell via other mechanisms. Unconventional Protein Secretion (UPS) comprises alternatives through which (1) leaderless proteins (lacking the signal sequence for ER localization) are secreted and (2) proteins that use the conventional secretory pathway take a different route, traversing from the ER straight to the plasma membrane [14,15]. Different types of UPS routes have been reported, each dealing with different types of stress [14,15]. Among the four types of UPS reported thus far, Types III and IV share the common participation of GRASPs [16-18]. In particular, Type III UPS is characterized by the formation of a new GRASP-rich organelle, named Compartment for Unconventional Protein Secretion (CUPS) [19], which leads the secretory protein to the plasma membrane, where vesicle fuses, releasing its cargo.

Our group has been exploring the biophysics of GRASPs in the last few years [20-25]. In one of our last contributions [22], we described novel structural features of Grh1, the GRASP from *Saccharomyces cerevisiae*. We have demonstrated that Grh1 contains regions of intrinsic disorder, which seems to be a common feature among GRASPs. Furthermore, it was shown that Grh1 formed amyloid-like fibrils *in vitro*, and the fibrillation was independent of its C-terminal domain [22]. *In vitro* fibrillation has been also observed for both human GRASPs and seems to be another general feature within the GRASP family [26,27]. A comprehensive review of the biophysics of GRASPs has been recently published [28].

The capacity of Grh1 to form amyloid fibrils is still of unclear biological significance. The presence of functional amyloid aggregates in yeast has been reported previously [2]. We hypothesized that the amyloid-like form of Grh1 also occurs *in vivo*, and the ensemble formed is closely related to the function of Grh1 in UPS, particularly in Type III during starvation [29], as well as upon increase in temperature (i.e., in Heat Shock Response - HSR) [30]. In the case of starvation, intracellular pH drops and becomes acidic [31], a condition that has been seen to trigger fibrillation *in vitro* [personal communication]. As for the temperature, we have recently reported fibrillation of Grh1 at temperatures greater than 37°C *in vitro* [22]. In the case of yeast, the optimal temperature for its growth is 30°C [30]. The cell can support mild temperature increases (for instance, from 37 to 41°C). HSR is a coordinated event that arrests cell growth through the aggregation of other proteins, thus impairing their function. This aggregation leads to the formation of Stress Granules (SG), which are

disassembled by Hsps when thermal stress ceases, and the cell returns to normal growth [30].

Here, we address one issue, namely Grh1 fibrillation *in vivo*, which has novelty for two reasons. On the one hand, detecting amyloid fibril formation *in vivo* is itself novel. Additionally, the demonstration of the formation of Grh1 fibrils inside the cell raises new insights toward better understanding the basic issues of UPS and HSR in yeast.

Results

Grh1 forms *in vitro* amyloid fibrils under different conditions

One of the main challenges in monitoring the fibrillation of a specific protein inside the cell is to find a suitable experimental method to detect fibril formation under the conditions of interest. Fluorescence Lifetime Imaging (FLIM) is based on the measurement of the time decay of the fluorescence signal after excitation at a determined wavelength and was the method of choice to first detect the autofluorescence of fibrils.

The formation of amyloid fibrils *in vitro* has been demonstrated for Grh1 [22]. In that study, it was shown that Grh1 fibrillates when submitted to either temperatures higher than 37 °C or to changes in the dielectric constant of the medium [22]. Those were two parameters intended to mimic Grh1 environment (or changes to it) in the cell, i.e. heat shock response and the presence of the membrane field, respectively. Here we complement that study by demonstrating that Grh1 also fibrillates when in acidic pH (≤ 5.5), a condition that has been shown to happen during starvation. We followed a similar protocol previously used [8] based on the autofluorescence of the fibrils detected using FLIM. The fluorescence decay times were also measured and used to distinguish changes in the fibril formation. The results are presented in Figure 1 and it is clearly seen that Grh1 indeed form fibrils in all tested conditions. Moreover, the structures formed upon heating or in acidic pH have different fluorescence time decays (the decay is slower in acidic pH), thus suggesting differences in the structure formed and/or in the microenvironment where the fibrils are formed. Therefore, the pH-induced fibrillation *in vitro* reinforces our hypothesis of fibrillation in starvation conditions in yeast.

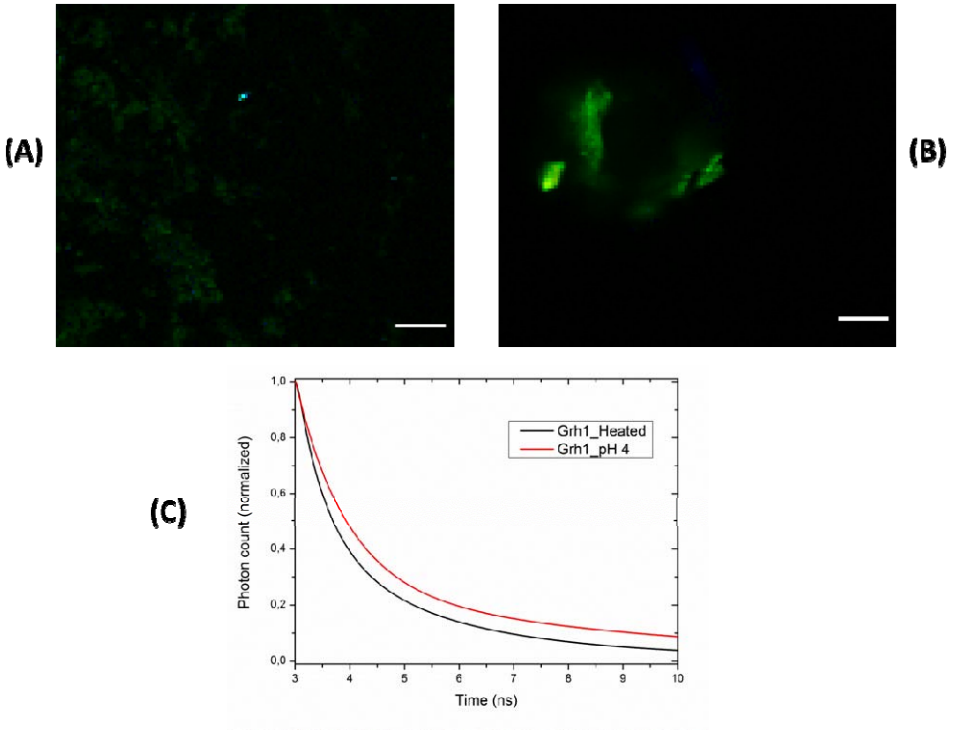

Figure 1: Grh1 fibrillates *in vitro* in different conditions. FLIM images of purified Grh1 excited at 375 nm. (A) Heated to 37°C. (B) At pH 4. (C) Time decays of fluorescence for heated Grh1 (black) and at pH 4 (red). Scale bar: 10 µM

Grh1 is capable of fibrillating in a cellular environment

After showing that Grh1 can form amyloid fibrils *in vitro* under conditions that correspond to stress scenarios in the cell, the natural step after that was to ask whether Grh1 could also form fibrils within the cell. Hence, following the same expression protocol described elsewhere [22], we initially turned to heterologously expressed Grh1 in *E. coli* so as to place Grh1 in a cellular environment. Here, the idea was to perform experiments as if we had exchanged the *in vitro* buffer used before for the *E. coli* cytoplasm.

Figure 2 shows the FLIM results obtained from *E. coli* cells after excitation at 375 nm at room temperature (Figure 2A), at 37°C (Figure 2B-C) and at pH 4.6 (Figure 2D). By using 20 mM sodium acetate in de LB medium as described by Wilks and Slonczewski [32], we were able to prevent the bacteria to regulate its internal pH, thus a decrease in LB pH will be translated into a decrease in the pH of the cytoplasm. The green background in all images is due to the medium autofluorescence. Rod-like

structures, resolved from the background autofluorescence and likely from Grh1, clearly appeared in the cell culture containing Grh1 heated at 37°C or in acidic pH (Figure 2C-D) (coloured in green and blue in Figure 2, where colours refer to lifetime values). We discarded random fibrillation due to protein overexpression by monitoring a negative control (Figure 2B), where the same *E. coli* strain overexpressing the non-amyloidogenic protein acyl-CoA binding protein (ACBP) did not show significant autofluorescence above the background signal. Controls in acidic pH did not show any signal either. Therefore, in the conditions that trigger *in vitro* fibrillation (increased temperature and acidic pH), Grh1 also fibrillates inside *E. coli.*

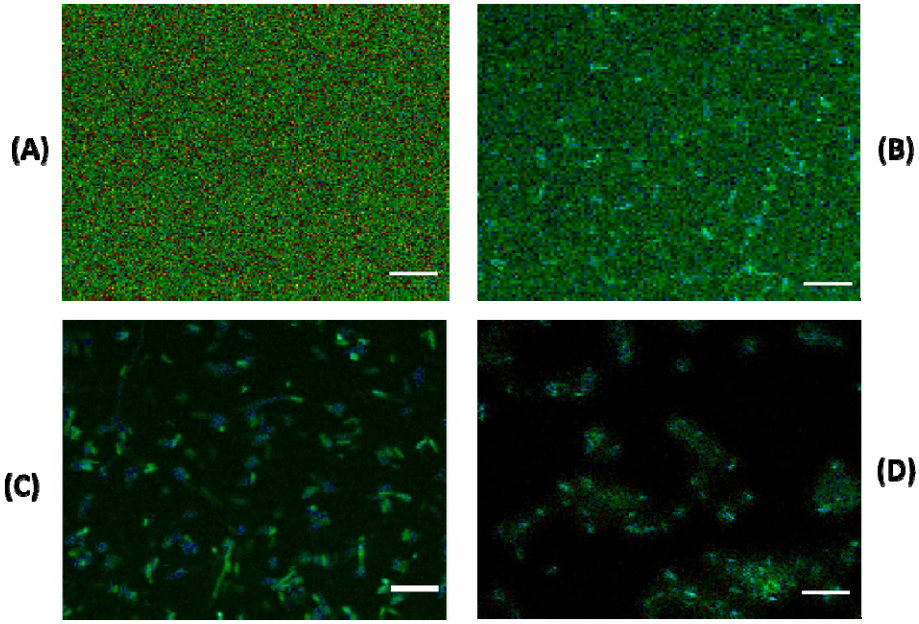

Figure 2: FLIM images of *E. coli* cells excited at 375 nm. The images show *E. coli* cells expressing: (A) Grh1 at room temperature. (B) ACBP in cells heated at 37°C after expression. (C) Grh1 in cells heated at 37°C. (D) Grh1 in cells in acidic medium. Scale bar: 10 µM.

Fibrillation in yeast under stress

In cell Grh1 fibrillation was also investigated in its native environment in *S. cerevisiae* again via FLIM experiments. It is suggested that fibrillation of Grh1 is related to stress, and conditions previously described to trigger UPS Type III [19] and HSR in yeast cells [27] were used. Figure 3 shows FLIM images obtained from a yeast strain called Y270, which does not carry any mutations in *grh1* or related genes and is hereafter referred to as Wild-type (WT) yeast. As expected, there is no autofluorescence

in the control cells (Figure 3C). Fluorescence is only observed when the cells are either heated at 37 ºC (Figure 3A) or submitted to starvation (Figure 3B), both being conditions known to trigger HSR and UPS Type III [27, 19], respectively.

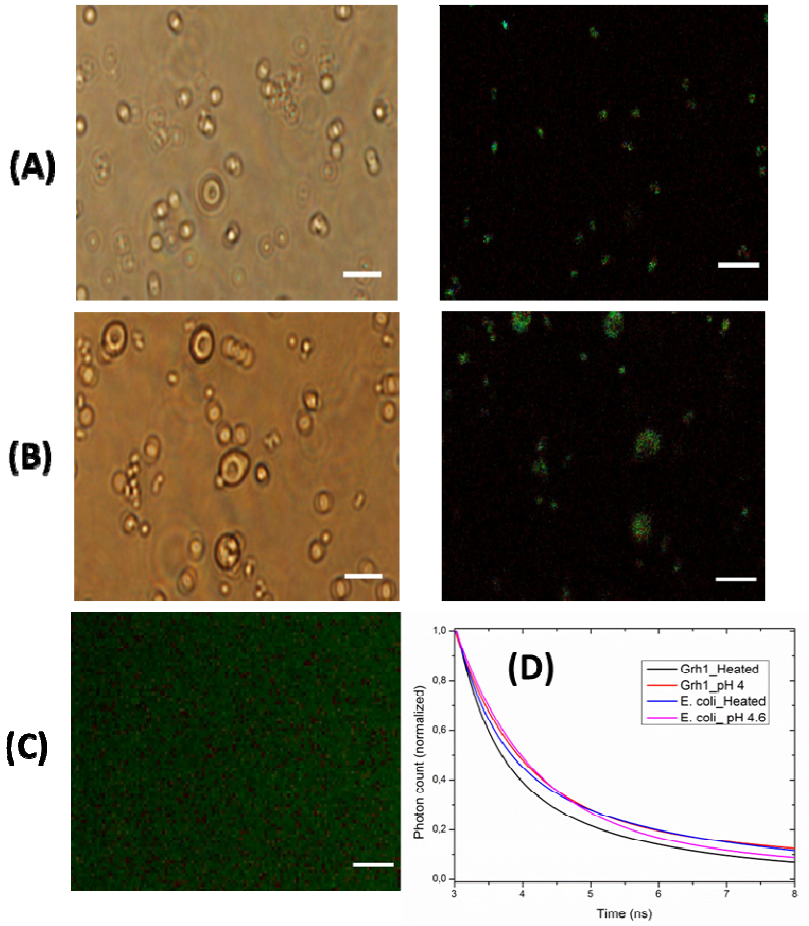

Figure 3: FLIM experiments with yeast cells excited at 375 nm: (A) Heated to 37°C. (B) Under starvation for at least 30 minutes. Left: bright field image. Right: FLIM image. (C) FLIM Image of Control sample. (D) Time decays of fluorescence for *E. coli* in pH 4.6 (black), heated *E. coli* (red), heated WT yeast (blue) and starved WT yeast (pink). Scale bar: 10 µM

Time decays of the fluorescence in yeast under either starvation or heated at 37°C were measured, and compared with those from heated *E. coli* overexpressing Grh1 and from *in vitro* experiments. In Figure 3D, the differences between *in cell* time decays of fluorescence are expected, since lifetime depends on the fluorophore environment [33]. Comparing the fluorescence decays of the different samples, temperature stress in both cell types (*E. coli* and yeast) led to identical time decays (Figure 3D). This

suggests differences in the environment of the fibrils upon temperature increase or during starvation, which is in agreement with the distinct responses of the cell to those stress conditions [19, 30].

The lack of Grh1 impairs fibrillation processes

The results shown in Figures 2 and 3 are indicative of *in cell* fibrillation of Grh1, but it could be argued that the fluorescence exhibited was due to other fibrillation processes taking place inside the cell. To better understand the origin of the observed fibrillation process, similar experiments were carried out, but this time with a Grh1 knockout yeast lineage.

As expected, under physiological conditions, no autofluorescence was observed. In the sample heated to 37°C (Figure 4A), however, there was a change in the pattern of fluorescence. Not only was the signal from Grh1 lost, but also the cells appeared as black dots. Although it was not possible to determine the loss of signal quantitatively from this experiment only, the events occurring in the cell suggest considerable changes took place in HSR when Grh1 was not present.

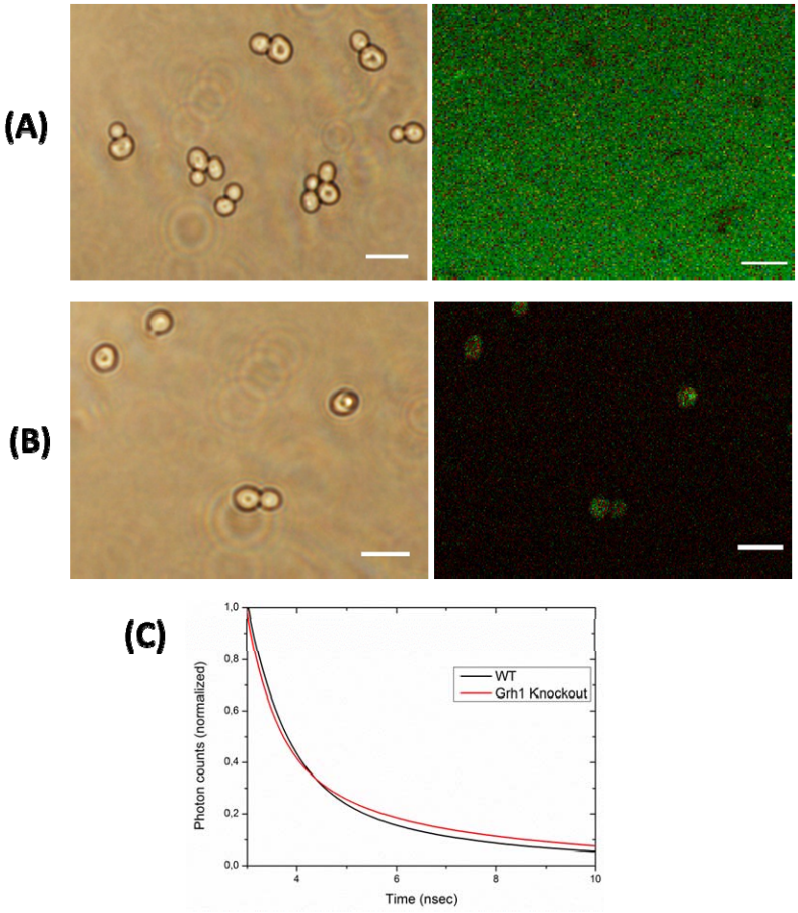

Figure 4: FLIM experiments with excitation at 375 nm. Grh1 knockout cells (A) heated to 37° C and (B) under starvation for at least 30 minutes. Left: bright field image. Right: FLIM image. (C) Time decays of fluorescence for WT (black) and Grh1 knockout (red). Scale bar: 10 µM

In starvation, some autofluorescence in the Grh1-knockout cells (Figure 4B) was observed. To investigate this somewhat unexpected result, we further examined the pattern, in terms of lifetime values (colors in Figures 3B and 4B), of fibrillation in both Grh1-containing and knocked-out yeast. In Figure 3B, a heterogeneous signal, containing a broader range of lifetime values (color pattern in the figure) was observed. On the other hand, in Figure 4B, the lifetime is very similar for all events. An explanation for such difference would be that in Figure 3B, other entities, besides Grh1, are also fibrillating in response to starvation. As Grh1 was removed (knockout cells), the color pattern seen in Figure 4B became more uniform because the contributions to fluorescence arising from the fibrils of Grh1 were no longer present. The decay of

fluorescence in both samples (Figure 4C) was also different, which confirms the contribution (or the absence of it) of Grh1 to the detected signal.

To further investigate fibrillation in starvation conditions, given that a signal in knockout cells was seen, we used a GFP-tagged strain and immunoprecipitated Grh1-GFP in a culture starved for 2 hours. Since an acidic pH was required for elution and that would give a false-positive result in the experiment, the complex beads-GFP-Grh1 was taken to the microscope and FLIM experiments performed. The results for the control and test conditions can be seen in Figure 5. In the immunoprecipitated sample from starved cells (Figure 5B) the signal that arises presents a decay that is very similar to that seen from the whole cells in starved conditions (Figure 5C). They both have the same slow lifetime (4.8±0.1 ns for the former and 5.0±0.4 ns for the latter). The different pre-exponential factors that led to the different decays suggest a reorganization caused by the potential release from CUPS, with fibrils more distant from each other. That is translated into a slightly slower decay.

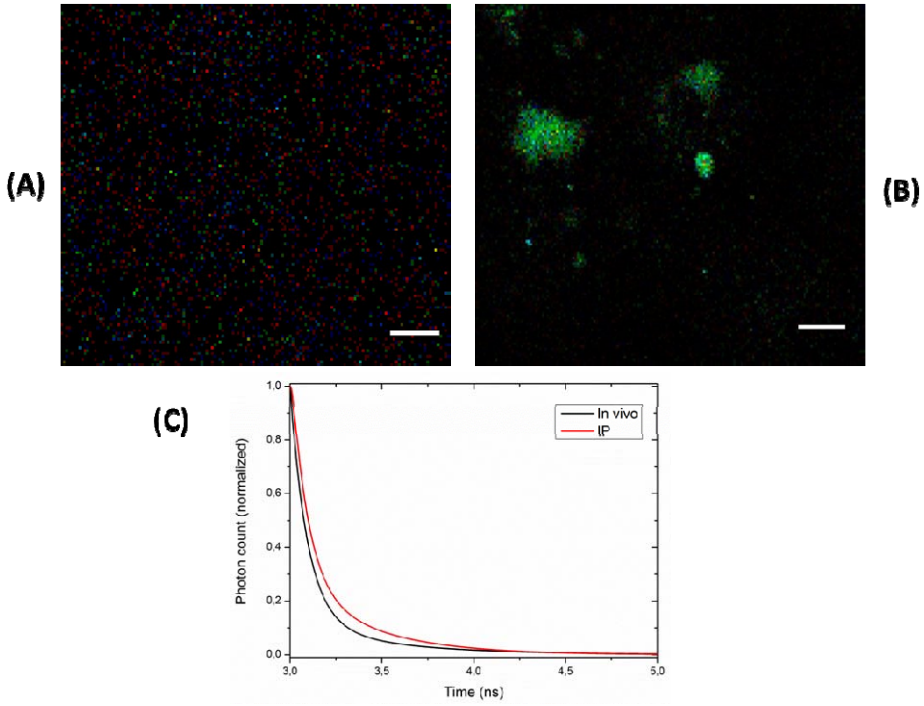

Figure 5: FLIM results from immunoprecipitation experiments with GFP-tagged strain: (A) control, (B) starvation, and (C) Decay of fluorescence for the GFP-tagged strain in starvation *in vivo* (black) and immunoprecipitated sample (red). Scale bar: 10 µM

Grh1 forms higher-order complexes in certain conditions

A different strategy to test the formation of large complexes is size exclusion chromatography (SEC), in which large complexes (in our case, fibrils) are excluded from the separation column. To trace the Grh1 movement, we employed the GFP-tagged Grh1 yeast strain. Yeast cells were cultivated under the desired condition: control, under starvation, or submitted to temperature increase. The whole extract obtained from disrupted yeast cells in each condition was then applied in a SuperDex200 and the proteins tracked via their optical absorbance at 280 and 395 nm for proteins and GFP, respectively. Figure 6A shows the results of SEC experiments using Grh1-GFP. For clarity, elution profiles were normalized and only the signal at 395 nm is shown. In the control experiment (black line), the signal from GFP appeared around 16 mL of elution. In starved cells (red line), the curve was shifted to the left, indicating that GFP (and consequently Grh1) was then too large to enter the column, being excluded at 9 mL. On the other hand, there were 2 populations in the non-permissive temperature condition (37 °C, blue line): one that was excluded from the column, and another that left the column at the same point as in the control condition. While SEC does not give information about the type of structure formed, it does indicate that, under stress conditions, Grh1 undergoes changes that significantly affect its size.

To explore whether the observed size change in Grh1 is due to protein aggregation, ultracentrifugation in SDS was used to differentiate amyloid fibrils from other possible amorphous aggregates of Grh1 [5]. We also used the Grh1-GFP strain and performed a dot blot (Figure 6B) to detect the presence of Grh1 in the non-solubilized pellet. Confirming the SEC observations, Grh1-GFP fibrils were present under stress conditions, but not in the control, indicating that Grh1 formed SDS-insensitive large complexes when the yeast cells were submitted to starvation or non-permissive temperature. We can therefore infer that the size increase was not due to amorphous aggregation, but rather to amyloid formation.

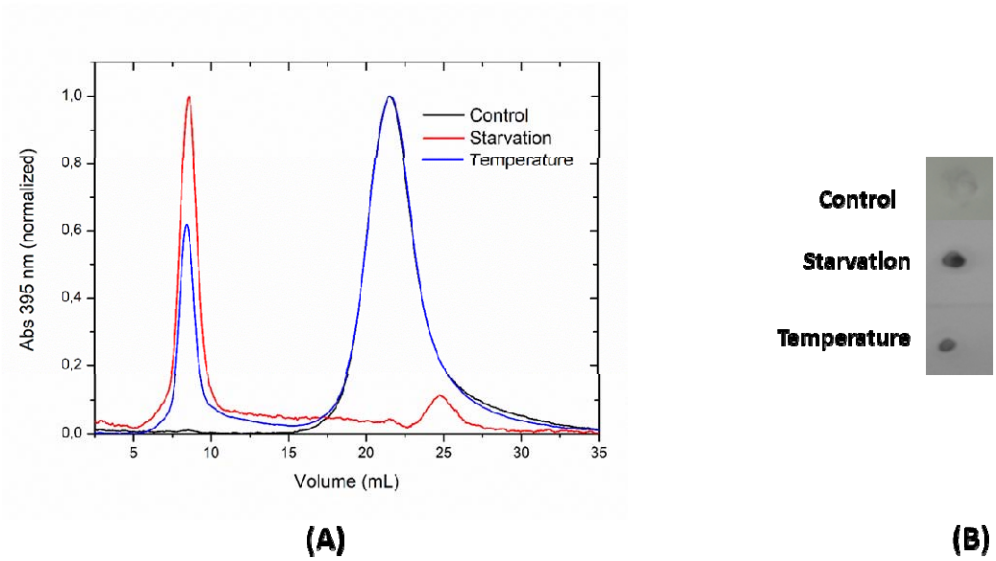

Figure 6: Experiments with Grh1-GFP strain. (A) Elution profile (normalized) of size exclusion chromatography following the GFP signal (395 nm). (B) Dot blot of the pellet obtained from the ultracentrifuged samples. The detection was based on the use of an anti-GFP antibody.

Fibrillation reversibility

After incubation in starvation conditions, yeasts are capable of returning to their normal state when physiological conditions are restored [29]. In agreement with that, our data show that there was no autofluorescence from the sample that was subjected to starvation for 2 hours and then brought back to normal conditions (Figure 7A), suggesting all the fibrillation events indicated by the autofluorescence in starvation conditions were reversible. Therefore, the fibrillation of Grh1 in this context seems to be reversible. Moreover, HSR is capable of sustaining the stress for 2 hours and the cells are able to go back to normal once optimal temperature is restored. Like starved cells, fluorescence from cells subjected to heating at 37°C for 2 hours (heat shock) was no longer seen when the cells were brought back to 30°C (Figure 7B).

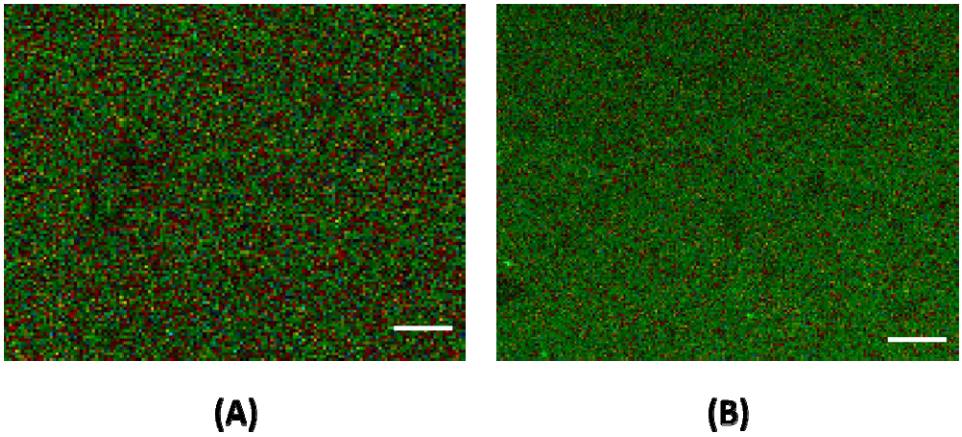

Figure 7: Reversibility experiments. FLIM experiments for cells submitted to (A) Starvation. (B) Heat-shock. Scale bar: 10 µM

Discussion

Detecting amyloid-like fibrils *in vivo* has proven to be a challenge. There are studies to detect aggregation within cells [5] that use chimeras of the target protein tagged with fluorescent reporters. Aggregation-prone proteins form foci inside the cells that can be visualized under the fluorescence microscope [5]. This approach can be very helpful, but in the case of Grh1, compartmentalization of the protein either in CUPS (in the case of starvation) or in what we suggest to be stress granules during HSR can lead to the formation of 1 to 3 punctate structures in Grh1 GFP-tagged strains, therefore hampering the direct identification of potential fibrils.

In 2013, Pinotsi *et al* [8] described for the first time a label-free assay for the detection of amyloid fibrils based on the intrinsic fluorescence in the UV-visible region that arises when the protein changes conformation and adopts the characteristic β-sheet rich structure of amyloids. Chan *et al* [9] further described this fluorescence signature and how unlikely it would be for an experiment based solely on fibril autofluorescence to be used *in vivo* due to competing autofluorescence from cells. It was not a surprise, then, the publications that followed using FLIM and intrinsic fluorescence were based on either FRET experiments or changes in a reporter's physicochemical parameter when fibrillation happened [10, 11]. Here, we used FLIM experiments to directly (without any extrinsic probe) detect Grh1-fibril autofluorescence as well as sedimentation and a

modified version of the filter retardation (in the form of a SEC experiment) assays [5] to further corroborate the FLIM data.

While it is understood that *in vivo* FLIM of proteins without a reporter may not always be possible, we were able to show (Figures 2, 3, and 4) this can be a valid approach for yeast cells. In control conditions, the fluorescence signal arising from the cells is negligible when excited at 375 (Figure 3C). On the other hand, there was a clear signal associated with the cells in stress conditions (Figures 3A and 3B). Furthermore, by using a Grh1-knockout strain and by comparing the lifetimes of fluorescence (Figure 4), we were able to establish Grh1 fibrillation through changes either in time decays/distribution (at 375 nm excitation) (Figure 4C) or by the lack of signal in the knockout strain (Figure 4A).

Amyloid formation inside cells has gained even more attention lately since now a number of aggregate-prone proteins have been described, especially in yeast, and the potential formation of amyloid-like structures of those proteins is not only disease-related [2]. Despite the challenge of following the kinetics of the formation of fibrils inside the cell without an extrinsic reporter, the autofluorescence itself can account not only for the detection of the fibrils (presence or absence – Figures 2, 3, and 4) but also for changes in the environment surrounding them (Figures 3A and 3B).

Grh1 fibrillation *in vitro* has been demonstrated [22], which may have significant implications for the cell because the fibrils are seemingly tools used to cope with different types of stress. Since our hypothesis was that fibrils of Grh1 were necessary under specific conditions, we tested *in vivo* fibrillation due to starvation or temperature-induced stress. In the former, Grh1 must leave the Golgi membrane and relocalize to be part of CUPS [16], whereas Grh1 is upregulated in heat shock [34].

Our experiments neither allowed for high-resolution structural determination of Grh1-containing assemblies nor permitted the exact location of fibrils inside the cells. However, we were able to detect, under stress stimuli, the formation of large molecular assemblies enriched in β-sheet. More specifically, we showed there is autofluorescence coming from the cell when either in starvation (Type III trigger – Figures 3B and 4B) or high temperature (HSR trigger – Figure 3A). While the signal for starvation has more than one component in the WT strain, we were able to dissect the contributions coming from Grh1. In the case of HS, the signal is lost in the absence of Grh1, suggesting deep

changes that are likely related to SG (Figure 4A). Furthermore, the time decays of fluorescence being different under different stimuli (Figure 3D) is a strong suggestion that the fibrils are in different environments, which is in accordance with the idea of distinct functions in each case. It might well be that, in starvation, the yeast would use Grh1 fibrils rather than their monomer to form CUPS, a finding that can offer novel ways to interpret Grh1 participation in UPS.

In summary, here we present solid evidence of *in vivo* formation of fibrils by Grh1 under stress conditions. While assumptions on how exactly they function in both Type III UPS and HSR are yet to be determined, our data reinforce the new concept of functional fibrils in yeasts as active factors in response to certain types of stress. As any first-time idea appearing in the literature, our findings seem to bring more questions than answers, but they surely offer new perspectives to better understand amyloids *in vivo* as well as Grh1 roles in UPS and HSR.

Materials and Methods

Protein Expression and Purification

The protocol for Grh1 expression in *E. coli* and purification is described elsewhere [22]. For the experiments with *E. coli* in acidic pH, cells were grown and expression was induced and carried out for 18 hours at 20 °C. Cells were pelleted by centrifugation at 8,000g for 10 minutes, and transferred for LB medium added of 50 mM MES and 20 mM sodium acetate, pH 4.6, and kept shaking at 20 °C for 1 hour.

Yeast Culture

The *Saccharomyces cerevisiae* strain Y470 was used in the FLIM experiments with excitation at 375 nm. All the other experiments without tagging or knockout were performed in the parental strain BY4741. The GFP-tagged and the knockout strains come from the commercial Yeast GFP clone collection (ThermoFisher Scientific). All cultures were grown in YPD medium (1% Yeast Extract, 2% Peptone, 2% Glucose).

For all experiments, a colony of the desired strain was placed in liquid YPD or SC-ura, and allowed to grow overnight at 30° C. The following morning the colony was

transferred to 200 ml of YPD, and allowed to grow again, this time under slow agitation until the culture reached an optical density at 600 nm of ca. 0.5.

For starvation, cultures were centrifuged and resuspended in 2% potassium acetate solution (as described by Cruz-Garcia *et al* [29]). For HSR, cultures were placed under agitation at 37 °C. Both experiments were run for 2 ½ hours, and the same time used for recovery, where the cultures were put back at optimal growth conditions.

Immunoprecipitation

Immunoprecipitation was carried out using the GFP-tagged strain, with the GFP-Trap Magnetic Agarose (Chromotek). Cells in the desired conditions were centrifuged at 12,000g for 10 minutes and the supernatant collected. The beads were previously equilibrated with dilution/washing buffer (10 mM Tris pH 7.5, 150 mM NaCl, 0.5 mM EDTA. pH adjusted to 8). Beads were added to the supernatant and the solution were left rotating end-to-end for 1 hour at 4 °C. Two washing steps were performed by separating the beads with a magnet until the supernatant was clear, discarding the supernatant and resuspending beads with washing buffer. Due to the pH-induced fibrillation previously observed for Grh1, the elution step was not performed and the beads with trapped GFP taken to the microscope.

Confocal and Fluorescence Lifetime Imaging Microscopies

FLIM experiments with excitation at 375 nm were performed in a PicoQuant MT 200 microscope. Emission was detected from 405 nm. Data collection and analysis was performed with the SymPhoTime 64 software (PicoQuant).

Gel Filtration

Cultures in different conditions were centrifuged and pelleted in PBS, followed by sonication during 7 minutes, in cycles of 30 sec on and 30 sec off. To separate solid particulates, cultures were centrifuged at 20,000g for 20 minutes, and the collected supernatant was concentrated using a Vivaspin column (GE Healthcare, Buckinghamshire, United Kingdom). The concentrated supernatant was applied to a Superdex200 10/300 GL gel filtration column (GE Healthcare, Buckinghamshire, United Kingdom).

Ultracentrifugation

2 mL of cultured cells were harvested and resuspended in 300 uL lysis buffer (50 mM Tris, pH 7.5, 150 mM NaCl, 2 mM EDTA, 1 mM PMSF, 5% glycerol). Disruption was carried out by vortexing with acid-washed glass beads. 300 µL of RIPA buffer (50 mM Tris, pH 7.0, 150 mM NaCl, 1% Triton X-100, 0.1% SDS) were added to the solution, which was vortexed again for 10 sec. Centrifugation at 1,500g for 5 minutes was used to pellet cell debris. 200 µL of the soluble fraction was centrifuged in a TLA 100-2 rotor for 45 min at 100,000g and 4 ºC in an Optima TL Beckman ultracentrifuge.

Dot Blot

10 µL of resuspended precipitate (see Ultracentrifugation) was blotted in nitrocellulose membrane, which was then blocked with Blocking buffer (TBST - 10 mM Tris, 150 mM NaCl, 0.1% Tween 20- plus 1% w/v BSA) for 24 hours. Incubation with rabbit-polyclonal anti-GFP primary antibody in a 1:10,000 dilution (Invitrogen Cat. Number #A-11122) in Blocking Buffer was carried out for one hour, followed by three washes with TBST. Incubation with anti-Rabbit Secondary Antibody Solution Alk-Phos. Conjugated (Invitrogen™) followed and preceded for one hour. Washing and detection were performed as recommended for Novex® AP Chromogenic Substrate.

Acknowledgments

The authors acknowledge Fundação de Amparo à Pesquisa do Estado de São Paulo (FAPESP) for the financial support (Grant no. 2015/50366-7, 2012/20367-3 and 2008/558316). NAF and ADR thank FAPESP for the PhD and undergraduate fellowships (Grant no. 2016/23863-2 and 2018/24968-8). AJCF thanks Conselho Nacional de Desenvolvimento Científico e Tecnlógico (CNPq) for the partial financial support (Grant no. 306682/2018-4). The authors also thank Prof. Cleslei Fernando Zanelli (Department of Biological Sciences, School of Pharmacy, UNESP, Brazil) for the Grh1 GFP-tagged and Grh1 knockout yeast strains.

Author contributions statement

NAF performed most of the experimental procedures and analyses. ADR was involved in part of the experimental procedures. AW and PSRC coordinated part of the project. AJCF conceived and coordinated the project. All authors also approved the final version of the manuscript.

Declaration of interests

The authors declare no competing interests.

References

[1] Koo, E. H., Lansbury, P. T., and Kelly, J. W. (1999) Amyloid diseases: Abnormal protein aggregation in neurodegeneration, *Proceedings of the National Academy of Sciences of the United States of America 96*, 9989-9990.

[2] Cereghetti, G., Saad, S., Dechant, R., and Peter, M. (2018) Reversible, functional amyloids: towards an understanding of their regulation in yeast and humans, *Cell Cycle 17*, 1545-1558.

[3] Iadanza, M. G., Jackson, M. P., Hewitt, E. W., Ranson, N. A., and Radford, S. E. (2018) A new era for understanding amyloid structures and disease, *Nature Reviews Molecular Cell Biology 19*, 755-773.

[4] Almeida, Z. L., and Brito, R. M. M. (2020) Structure and Aggregation Mechanisms in Amyloids, *Molecules 25,5 1195*.

[5] Alberti, S., Halfmann, R., and Lindquist, S. (2010) BIOCHEMICAL, CELL BIOLOGICAL, AND GENETIC ASSAYS TO ANALYZE AMYLOID AND PRION AGGREGATION IN YEAST, *Methods in Enzymology, Vol 470: Guide to Yeast Genetics:: Functional Genomics, Proteomics, and Other Systems Analysis, 2nd Edition 470*, 709-734.

[6] Elghetany, M. T., and Saleem, A. (1988) METHODS FOR STAINING AMYLOID IN TISSUES - A REVIEW, *Stain Technology 63*, 201-212.

[7] Reiman, E. M., and Jagust, W. J. (2012) Brain imaging in the study of Alzheimer's disease, *Neuroimage 61*, 505-516.

[8] Pinotsi, D., Buell, A. K., Dobson, C. M., Schierle, G. S. K., and Kaminski, C. F. (2013) A Label-Free, Quantitative Assay of Amyloid Fibril Growth Based on Intrinsic Fluorescence, *Chembiochem 14*, 846-850.

[9] Chan, F. T. S., Schierle, G. S. K., Kumita, J. R., Bertoncini, C. W., Dobson, C. M., and Kaminski, C. F. (2013) Protein amyloids develop an intrinsic fluorescence signature during aggregation, *Analyst 138*, 2156-2162.

[10] Esbjorner, E. K., Chan, F., Rees, E., Erdelyi, M., Luheshi, L. M., Bertoncini, C. W., Kaminski, C. F., Dobson, C. M., and Schierle, G. S. K. (2014) Direct Observations of Amyloid beta Self-Assembly in Live Cells Provide Insights into Differences in the Kinetics of A beta(1-40) and A beta(1-42) Aggregation, *Chemistry & Biology 21*, 732-742.

[11] Schierle, G. S. K., Bertoncini, C. W., Chan, F. T. S., van der Goot, A. T., Schwedler, S., Skepper, J., Schlachter, S., van Ham, T., Esposito, A., Kumita, J. R., Nollen, E. A. A., Dobson, C. M., and Kaminski, C. F. (2011) A FRET Sensor for Non-Invasive Imaging of Amyloid Formation in Vivo, *Chemphyschem 12*, 673-680.

[12] Barr, F. A., Puype, M., Vandekerckhove, J., and Warren, G. (1997) GRASP65, a protein involved in the stacking of Golgi cisternae, *Cell 91*, 253-262.

[13] Viotti, C. (2016) ER to Golgi-Dependent Protein Secretion: The Conventional Pathway, In *Methods in Molecular Biology*, pp 3-29, Humana Press, New York.

[14] Rabouille, C., Malhotra, V., and Nickel, W. (2012) Diversity in unconventional protein secretion, *Journal of Cell Science 125*, 5251-5255.

[15] Nickel, W., and Rabouille, C. (2009) Mechanisms of regulated unconventional protein secretion, *Nature Reviews Molecular Cell Biology 10*, 148-155.

[16] Giuliani, F., Grieve, A., and Rabouille, C. (2011) Unconventional secretion: a stress on GRASP, *Current Opinion in Cell Biology 23*, 498-504.

[17] Brough, D., Pelegrin, P., and Nickel, W. (2017) An emerging case for membrane pore formation as a common mechanism for the unconventional secretion of FGF2 and IL-1 beta, *Journal of Cell Science 130*, 3197-3202.

[18] Malhotra, V. (2013) Unconventional protein secretion: an evolving mechanism, *Embo Journal 32*, 1660-1664.

[19] Cruz-Garcia, D., Malhotra, V., and Curwin, A. J. (2018) Unconventional protein secretion triggered by nutrient starvation, *Seminars in Cell & Developmental Biology 83*, 22-28.

[20] Mendes, L. F. S., Garcia, A. F., Kumagai, P. S., de Morais, F. R., Melo, F. A., Kmetzsch, L., Vainstein, M. H., Rodrigues, M. L., and Costa, A. J. (2016) New structural insights into Golgi Reassembly and Stacking Protein (GRASP) in solution, *Scientific Reports 6, 29976*.

[21] Mendes, L. F. S., Basso, L. G. M., Kumagai, P. S., Fonseca-Maldonado, R., and Costa, A. J. (2018) Disorder-to-order transitions in the molten globule-like Golgi Reassembly and Stacking Protein, *Biochimica Et Biophysica Acta-General Subjects 1862*, 855-865.

[22] Fontana, N. A., Fonseca-Maldonado, R., Mendes, L. F. S., Meleiro, L. P., and Costa, A. J. (2018) The yeast GRASP Grh1 displays a high polypeptide backbone mobility along with an amyloidogenic behavior, *Scientific Reports 8, 15690*.

[23] Mendes, L. F. S., Fontana, N. A., Oliveira, C. G., Freire, M., Lopes, J. L. S., Melo, F. A., and Costa-Filho, A. J. (2019) The GRASP domain in golgi reassembly and stacking proteins: differences and similarities between lower and higher Eukaryotes, *Febs Journal 286*, 3340-3358.

[24] Reddy, S. T., Mendes, L. F. S., Fontana, N. A., and Costa, A. J. (2019) Exploring structural aspects of the human Golgi matrix protein GRASP55 in solution, *International Journal of Biological Macromolecules 135*, 481-489.

[25] Mendes, L. F. S., Batista, M. R. B., Judge, P. J., Watts, A., Redfield, C., and Costa, A. J. (2020) Conformational flexibility of GRASPs and their constituent PDZ subdomains reveals structural basis of their promiscuous interactome, *Febs Journal 287*, 3255-3272.

[26] Reddy, S. T., Uversky, V. N., and Costa-Filho, A. J. (2020) Biophysical characterization of intrinsically disordered human Golgi matrix protein GRASP65, *Int J Biol Macromol 162*, 1982-1993.

[27] Reddy, T. S., Uversky, V. N., and Costa-Filho, A. J. (2020) Nucleation-dependent amyloid fibrillation of human GRASP55 in aqueous solution, *Eur Biophys J. 49(2)*, 133-143.

[28] Mendes, L. F. S., Fontana, N. A., Reddy, S. T., Uversky, V. N., and Costa-Filho, A. J. (2020) The exquisite structural biophysics of the Golgi reassembly and stacking proteins, *Int J Biol Macromol*. 164, 3632-3644.

[29] Cruz-Garcia, D., Curwin, A. J., Popoff, J. F., Bruns, C., Duran, J. M., and Malhotra, V. (2014) Remodeling of secretory compartments creates CUPS during nutrient starvation, *Journal of Cell Biology 207*, 695-703.

[30] Lindquist, S. (1986) THE HEAT-SHOCK RESPONSE, *Annual Review of Biochemistry 55*, 1151-1191.

[31] Orij, R., Postmus, J., Ter Beek, A., Brul, S., and Smits, G. J. (2009) In vivo measurement of cytosolic and mitochondrial pH using a pH-sensitive GFP derivative in Saccharomyces

cerevisiae reveals a relation between intracellular pH and growth, *Microbiology (Reading) 155*, 268-278.

[32] Wilks, J. C., and Slonczewski, J. L. (2007) pH of the cytoplasm and periplasm of Escherichia coli: rapid measurement by green fluorescent protein fluorimetry, *J Bacteriol 189*, 5601-5607.

[33] Jain, A., Blum, C., and Subramaniam, V. (2009) Fluorescence lifetime spectroscopy and imaging of visible fluorescent proteins In *Advances in Biomedical Engineering* (P., and Verdonck, Eds.), pp 147-176, Elsevier, Amsterdam.

[34] Venters, B. J., Wachi, S., Mavrich, T. N., Andersen, B. E., Jena, P., Sinnamon, A. J., Jain, P., Rolleri, N. S., Jiang, C. Z., Hemeryck-Walsh, C., and Pugh, B. F. (2011) A Comprehensive Genomic Binding Map of Gene and Chromatin Regulatory Proteins in Saccharomyces, *Molecular Cell 41*, 480-492.